Flow of Quasi-Two Dimensional Water in Graphene Channels

Chao Fang, Xihui Wu, Fengchang Yang, and Rui Qiao*

Department of Mechanical Engineering, Virginia Tech, Blacksburg, VA 24061, USA

ABSTRACT: When liquids confined in slit channels approach a monolayer, they become two-dimensional (2D) fluids. Using molecular dynamics simulations, we study the flow of quasi-2D water confined in slit channels featuring pristine graphene walls and graphene walls with hydroxyl groups. We focus on to what extent the flow of quasi-2D water can be described using classical hydrodynamics and what are the effective transport properties of the water and the channel. First, the in-plane shearing of quasi-2D water confined between pristine graphene can be described using the classical hydrodynamic equation, and the viscosity of the water is ~%50 higher than that of the bulk water in the channel studied here. Second, the flow of quasi-2D water around a single hydroxyl group is perturbed at distance to tens of cluster radius from its center, as expected for low Reynolds number flows. Even though water is not pinned at the edge of the hydroxyl group, the hydroxyl group screens flow greatly, with a single, isolated hydroxyl group rendering drag similar to ~90nm^2 pristine graphene walls. Finally, the flow of quasi-2D water through graphene channels featuring randomly distributed hydroxyl groups resembles the fluid flow through porous media. The effective friction factor of the channel increases linearly with the hydroxyl groups' area density up to 0.5nm^{-2} but increases nonlinearly at higher densities. The effective friction factor of the channel can be fitted to a modified Carman equation at least up to a hydroxyl area density of 2.0nm^{-2}. These findings help understand the liquid transport in 2D material-based nanochannels for applications including desalination.

* To whom correspondence should be addressed. Email: ruiqiao@vt.edu

I. Introduction

Fluid transport in nano-channels/pores, or nanofluidic transport, has attracted great attention in recent years because of its role in applications including biochemical analysis, desalination, and energy storage.[1, 2, 3, 4, 5, 6, 7, 8, 9, 10] Because the critical dimension of nanochannels can be comparable to the intrinsic length scale of the working fluids (e.g., fluid molecule's diameter and/or the Debye length of electrolytes), the properties of fluids in the channel can deviate from those of bulk fluids. For example, compared to bulk water, water confined in the nano-gaps between mica surfaces shows enhanced viscosity[11] while water confined in carbon nanotubes (CNTs) with diameter <1.5nm shows reduced viscosity.[12] Furthermore, classical hydrodynamic theories can break down in nanochannels. For instance, molecular dynamics (MD) simulations revealed that the classical Navier-Stokes equations break down for the flow of Lennard-Jones fluids in slit channels with a width less than about four fluid molecule diameters.[13] When the fluids confined in nanopores are subject to shearing with wavelength comparable to fluid molecules' diameter, the local constitutive law relating shear stress and strain rate (thus the classical hydrodynamic theories) breaks down and flow must be described using the generalized hydrodynamic theories.[14, 15]

Most of the existing work on nanofluidic transport focuses on situations in which the critical dimension of the channel is larger than a few fluid diameters because even narrower channels are difficult to fabricate. Therefore, fluids in the nanochannels are still three dimensional in nature and much of nanofluidic research focuses on the flow behavior (e.g., velocity profile) across the channels. Such a situation, however, is being changed due to the emergence of two-dimensional (2D) materials such as graphene. By stacking 2D materials together and controlling the spacing between them, it is possible to prepare slit-shaped nanochannels with size comparable to fluid molecules' size and these channels have shown promise in applications such as desalination.[16, 17] Study of the fluid transport in the slit channels formed by 2D materials has become a fast moving front in nanofluidic research and interesting results have been reported.[18, 19, 20, 21] For example, water viscosity is found to fluctuate as a function of the width of the channel formed by pristine graphene layers.[22]

A unique aspect of the slit nanochannels formed by the 2D materials is that, when the channel width is comparable to the size of a fluid molecule, the fluids in the channels exist as a monolayer or a quasi-monolayer. In such situations, the fluids can hardly be considered as three-dimensional

entities as in wide channels, and they are better viewed as 2D or quasi-2D entities. The transport behavior of such 2D fluids has only begun to be studied recently.[19, 20, 22, 23] For example, it was found that a 2D network of water molecules can form between pristine graphene patches of the nanochannels built from graphene oxide (GO) sheets and such network can enhance water permeation through nanochannels.[17] While these studies advanced the fundamental understanding of the transport of 2D or quasi-2D fluids, many questions remain to be addressed.

One of the key issues for the 2D or quasi-2D fluids is how to describe their flow effectively. Although one can still treat the flow of these fluids in a 3D manner (e.g., it is possible to compute their velocity profile across slit channels in the z-direction), it is desirable to treat the flow as 2D flow and use the velocity averaged in the z-direction to describe the flow, given that the fluids are nearly a monolayer. However, it is not yet clear whether the classical hydrodynamic models hold for such flow and what transport properties should be used in the models. For example, 2D fluids are often subject to shearing in directions parallel to the channel wall (i.e., in-plane shearing). Can flow subject to such shearing be modeled using continuum hydrodynamics? If yes, what shear viscosity should be used in the model? In addition, functionalization groups are often found on 2D materials' surface (e.g., hydroxyl groups are often found on graphene surfaces),[24] and they have been shown to reduce transport of water through nanochannels by reducing the slip length at the graphene-water interfaces.[19, 20, 25] However, a detailed picture of the flow around functionalization groups is lacking at present, and it is not clear whether the features of these flows are similar to those expected from classical continuum hydrodynamics. For the even more complicated scenario where many functionalization groups exist on the channel walls, it is desirable to understand the overall hydrodynamic behavior of the channel (e.g., what is the drag rendered by the channel to the fluids) and describe how such overall behavior depends on properties such as the area density of the functionalization groups on the channel walls.

In this study, we use molecular dynamics (MD) simulations to investigate the flow of water in subnanometer-wide graphene channels. We first investigate the in-plane shearing of the quasi-2D water in pristine graphene channels. We examine whether such flow can be described by the classical hydrodynamic models when the water-wall friction is taken into account and determine the shear viscosity of the quasi-2D water. We next study the flow of quasi-2D water near single and small cluster of hydroxyl groups on the graphene walls. We examine how the flow is perturbed

by the hydroxyl groups and the accompanying drag force. Finally, we study the flow of quasi-2D water through graphene channels featuring randomly distributed hydroxyl groups. We examine how the drag force exerted by the channel to the water varies with the area density of the hydroxyl groups and whether such drag can be described using the empirical formula for fluid drag in porous media. The rest of this manuscript is organized as follows. In Section II, the molecular model and simulation details are presented. In Section III, the structure, dynamics, and hydrodynamics of quasi-2D water confined in channels with pristine and hydroxyl-functionalized graphene as walls are discussed. Finally, conclusions are drawn in Section IV.

II. Computational Details

Molecular systems. Figure 1 shows snapshots of the MD systems used for studying the flow of quasi-2D water in graphene channels. In Fig. 1a, the channel walls are pristine graphene layers; in Fig.1b, the channel walls feature hydroxyl groups (either forming a cluster or randomly distributed). All graphene sheets have the same lateral (*xy*-) dimension of $6.30\times6.06\text{nm}^2$ unless otherwise mentioned, and the system is periodic in all three directions. The channel width W is defined as the center-to-center distance between the carbon atoms in the two graphene walls. To model channels that are periodic only in the *xy*-plane, a 4nm-thick vacuum space is placed between the graphene channel and its periodical images in *z*-direction, and the electrostatic interactions are computed using the slab-PME method (see below). The channel width is 0.85nm. This channel width is adopted to ensure that water is a quasi-two dimensional (quasi-2D) liquid in the graphene channel. To meet this requirement, firstly, the channel must not contain more than one distinct layer of water molecules, which sets the upper bound of pore width to ~0.9nm. Secondly, water must not crystalize into a solid in the channel. Previous researches showed that water is prone to form ice in channels with a width of ~0.65-0.75nm.[23, 26] Therefore, the channel width should be 0.75-0.9nm in our study. Because we are primarily interested in general features of the flow of quasi-2D water, a channel width of 0.85nm is adopted. With this width, water molecules in the channel exist as a quasi-monolayer (see below) and behave as quasi-2D fluids. A channel width of 0.80nm is also used in some simulations and the results are qualitatively similar to that obtained from the 0.85nm-wide channel (see Section III.B).

The number of water molecules in each channel is determined using grand canonical MD simulations. In these simulations, the graphene channels shown in Fig. 1 are connected to two large

water reservoirs in which the pressure is maintained by pistons (see Fig. S2 in the Supplementary Material). The graphene channels are initially empty and equilibration runs of 10 ns are performed. Typically, the systems reach equilibrium in less than 5ns. The number of water molecules inside the channel during the last 5ns is used to compute the equilibrium density of water molecules per unit projection area of the graphene walls in *xy*- plane, and the results are summarized in Table S1 of the Supplementary Material. The channels in Fig. 1a and 1b are then filled with water molecules based on the equilibrium water density thus computed.

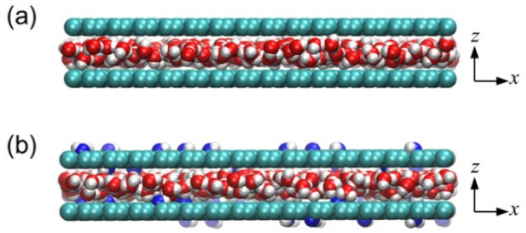

Figure 1. The side-view snapshots of the molecular systems for studying the structure and flow of quasi-2D water in slit channels with pristine graphene walls (panel **a**) and graphene walls functionalized with hydroxyl groups (panel **b**). The systems are periodic in all directions and the spacing between graphene walls is 0.85nm. The red, blue, white, and cyan spheres denote water oxygen, hydroxyl oxygen, hydrogen, and carbon atoms, respectively. 3D-view snapshots of the systems are shown in Fig. S1 in the Supplementary Material.

Molecular models. Both pristine graphene walls and graphene walls decorated with hydroxyl groups have been used in the MD simulations. To build graphene walls with hydroxyl groups, oxidized carbon atoms are either randomly distributed on the graphene walls to obtain the target density of hydroxyl groups or clustered together with molecular separations on one graphene wall (see Section III). All carbon atoms are fixed during each simulation,[18, 19, 21, 27] but the oxygen and hydrogen atoms are allowed to move to account for the flexibility of the surface groups. The bond stretching, angle bending, and torsional bending of the hydroxyl groups (including hydrogen, oxygen, and connected carbon atoms) are all taken into account explicitly. This vibration of the hydroxyl groups has little effect on its average position in the *z*-direction (e.g., the center of mass position of the hydroxyl group varies less than 0.01nm in the simulations) and it does not greatly alter the water flow in the graphene channel.

The OPLS-AA force fields[28], which are widely used to model graphene with surface groups,[20, 21] are adopted to describe the graphene and the hydroxyl groups. The rigid SPC/E model[28] is used

for the water molecules. The force field parameters including non-bonded Lennard-Jones potential and bonded interactions are listed in the Supplementary Material.

Simulation methods. Two types of simulations have been performed. First, non-equilibrium simulations are performed to study the flow of quasi-2D water confined in the graphene channels. As practiced in numerous studies of fluid transport in nanochannels, the flow is driven by a constant acceleration applied on fluid molecules in the x-direction.[20, 29, 30, 31] The accelerations are selected such that the resulting velocity of water molecules is less than 25m/s and the water velocity varies linearly with the applied acceleration. The latter ensures that the results obtained here can be safely extrapolated to practical operating conditions where the driving force (and hence the water velocity) is much smaller than that used in MD simulations. Second, equilibrium simulations are performed to study the dynamics of water molecules in the graphene channels. All simulations are performed in the NVT ensemble (T=300K) using the Gromacs code.[32] The water temperature is maintained using the velocity-rescaling thermostat.[33] We find that other choices of thermostat and thermostatting strategy lead to flow behaviors very similar to those reported here (see Supplementary Material). A cutoff of 1.2nm is used for computing the Lennard-Jones potential and the particle mesh Ewald method with a slab correction[34, 35] is used to calculate the electrostatic interactions.

The validity of the above methods has been examined by studying the slippage of water on pristine graphene walls. Specifically, a 4.0nm-wide graphene channel is filled with water and a flow is induced by applying an acceleration of 1.0×10^{-5}nm/ps^2 in the x-direction. From the computed velocity profile, we obtain a slip length of 59.3nm on the graphene surface, which agrees well with that reported in previous simulations.[36]

III. Results and Discussion

A. Quasi-two dimensional water in graphene channels

Figure 2a shows the density profile of water across a 0.85nm-wide slit channel with pristine graphene walls. The number density of water is higher than that in bulk water (~33.3nm^{-3}) in the central portion of the channel and two weak peaks appear near the graphene walls due to the layering of water.[20, 27] However, the water density at the channel center is only ~35% lower than those at the density peaks. Therefore, water molecules in the channel form a structure intermediate

between a clear monolayer and a distinct bilayer. To clarify the structure of the water inside the channel further, we examine how water molecules in the channel are coordinated by each other. Figure 2b shows the water number density distribution around a central water molecule located at 0.335nm above the lower channel wall (i.e., at the density peak marked by a magenta circle in Fig. 2a and Fig. 2b). We observe that this water molecule is mostly coordinated by the water molecules near the lower channel wall, and coordination by water molecules in the layer near the upper channel wall is limited. This suggests that the water in channel is closer to a monolayer than to a bilayer. The water structure revealed in Fig. 2a and 2b, along with the fact that flow observables such as velocity shows little variation across the channel in the *z*-direction (see below), suggests that the water in the channel can be considered as quasi-2D liquids.

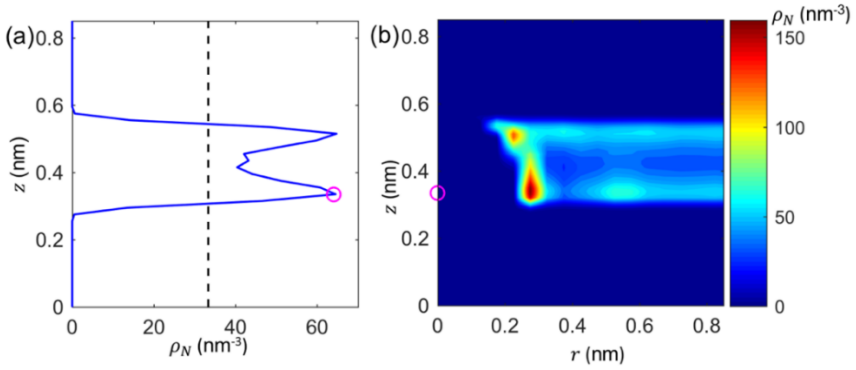

Figure 2. *The structure of the quasi-two dimensional* (*2D*) *water between two pristine graphene walls.* (**a**) Water number density distribution across the channel (*z*-direction). The two graphene sheets are located at z=0 and 0.85nm. The number density of bulk water is shown as a dashed line. (**b**) Number density of the water molecules around a central water molecule located at the density peak near lower graphene wall in panel **a.** The position of this central water molecule is labeled using a magenta circle in both **a** and **b**. *r*- is the radial direction in the horizontal (*xy*-) plane and it emanates from the central water molecule.

B. In-plane shearing of quasi-2D water

For quasi-2D water confined inside slit channels, its flow often involves shearing in the horizontal plane (termed in-plane shearing hereafter). For example, in channels formed by graphene layers, their walls often include both pristine patches and patches with hydrophilic surface groups.[37, 38] Since flow is significantly retarded within the hydrophilic patches (termed "side pinning" by Xu and colleagues[20]), there exists significant velocity gradient in the horizontal plane and consequently substantial shearing of water in the in-plane direction. For 2D or quasi-2D liquids confined in the pristine patches of the channels, where their shearing due to the velocity

gradient in the across-channel (z-) direction is negligible, such in-plane shearing greatly affects the liquid flux through the channel.

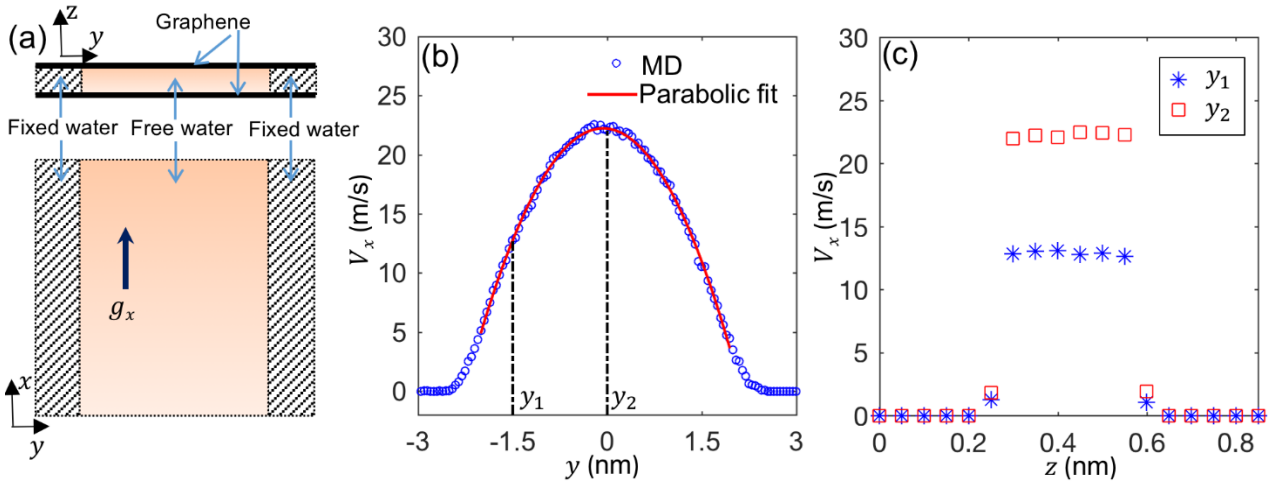

Figure 3. *In-plane shearing of quasi-2D water confined in 0.85nm-wide pristine graphene channels.* (**a**) Side- and top-views of the MD system. Water molecules within 0.5nm from the left and right edge of the simulation box (the shaded regions) are fixed to mimic the side pinning of water by the hydrophilic patches of graphene walls. A constant acceleration along the x-direction is applied to each water molecule to drive the flow and generate in-plane shearing of the water. (**b**) The water velocity profile along the y-direction. (**c**) The water velocity profile in the cross-channel (z-) direction at positions y_1 and y_2 labeled in panel **b**.

To probe the in-plane shearing of water, we freeze two strips of water molecules in the graphene channel as shown in Fig. 3a. Note the system is first equilibrated for 10ns before freezing water molecules in the two strips. These two strips of water molecules, each measuring 0.5nm wide in the y–direction, effectively create a no-slip boundary condition for the water flowing along the channel walls. Next, a constant acceleration of g_x=10^{-2}nm/ps^2 is applied on all other water molecules in the channel to drive flow in the x-direction. We verify that the flow is in the linear response regime. Figure 3b shows the distribution of water velocity normal to the fixed water strip (i.e., across the y-direction). A parabolic velocity profile is observed in the central portion of the channel, similar to the force-driven flow in macroscale slit channels. Figure 3c shows the distribution of the velocity of water molecules located at $y = -1.5$nm and 0nm in the cross-channel (z-) direction. The variation of water velocity across the channel is small, further suggesting that it is reasonable to consider the water inside the channel as quasi-2D fluids.

The parabolic velocity profile shown in Fig. 3b suggests that the classical hydrodynamic model can be applied for the flow of quasi-2D water. To predict the flow of quasi-2D water using classical

hydrodynamics, one must determine their transport properties. Here, we extract the viscosity of the quasi-2D water from the velocity profile shown in Fig. 3b. To this end, we construct a continuum model for the flow in channels shown in Fig. 3a by treating the fluids inside the channel as a 2D object. First, we assume that the in-plane shear stress is given by $\tau_x = \mu dV_x/dy$, where μ is the dynamic viscosity for in-plane shearing and V_x is the water velocity. Note that, in 2D space, the shear stress is a line stress and dynamic viscosity is related to the kinematic viscosity ν by $\mu = \rho_a \nu$ where ρ_a is the area density of 2D fluids. Next, the drag rendered by the stationary graphene walls to the water is modeled as a body force $F_b = f_{w,pris}V_x$ ($f_{w,pris}$ is the friction factor of pristine graphene channel and its calculation is presented in the Supplementary Material). It follows that, for a flow driven by a constant acceleration in the *x*-direction, its governing equation is

$$\rho_a \nu \frac{d^2}{dy^2} V_x(y) + \rho_a g_x - f_{w,pris} V_x(y) = 0 \quad (1)$$

For the system shown in Fig. 3a, $\rho_a = 3.90 \times 10^{-7}$kg/m^2. Separate simulations determined that the wall friction factor for the water enclosed between the graphene walls is $f_{w,pris} = 1.23 \times 10^4$ Pa·s/m (see Supplementary Material). Since the maximal $V_x(y)$ is ~20m/s in the channel and $g_x = 10^{-2}$nm/ps^2, $f_{w,pris}V_x$ is at least 15 times smaller than $\rho_a g_x$ anywhere in the channel and thus this term can be neglected safely for the flow shown in Fig. 3b. With the no-slip boundary condition at the edge of the fixed water molecules ($y = \pm 2.5$nm in Fig. 3a), the water velocity profile is parabolic and its curvature at the middle line of the horizontal plane (*y*=0) is g_x/ν. Using the fitted parabolic curve shown in Fig. 3b, a kinematic viscosity of ν =1.09×10^{-6}m^2/s is obtained for the quasi-2D water confined in the pristine graphene channel with a width of *W*=0.85nm. We note that the in-plane shearing viscosity obtained here is higher than bulk viscosity and is sensitive to the channel width. We find that the viscosity corresponding to the in-plane shearing of water in 0.80nm-wide channels is ~33% higher than that in 0.85nm-wide channels. The higher viscosity than that in bulk and the increase of viscosity as the channel width reduces in the range of widths examined here are similar to that reported in prior work.[22] In that work, water molecules were packed into graphene channels with prescribed densities, the Green-Kubo formulism was used to compute the viscosity of water, and the graphene was modeled using the reaxFF force fields. The facts that different simulation protocols, methods of viscosity calculation, and graphene force

fields lead to similar phenomenon suggest that the phenomenon observed here is robust and insensitive to computational details.

The kinematic viscosity of the quasi-2D water computed above is 50% higher than the kinematic viscosity of bulk SPC/E water at 300K (0.72×10^{-6}m^2/s).[39] To understand the origins of the enhanced viscosity of the quasi-2D water, we look into the structure and dynamics of quasi-2D water confined in 0.85nm-wide graphene channels. Figure 2b shows that the coordination of water molecules in these channels by other molecules is strongly affected by the confinement. We examine the hydrogen bonding between water molecules in this graphene channel, as it is a key aspect of water-water coordination and greatly affects the viscosity of water. To identify hydrogen bonds, we adopt the geometrical criteria,[40] i.e., $L_{o-o} \leq 0.35$nm and $\angle OOH \leq 30^o$ (L_{o-o}: oxygen-oxygen distance; $\angle OOH$: angle formed between one water molecule's OH bond and the oxygen-oxygen vector pointing from the donor to the acceptor). On average, each water molecule in the channel is coordinated by 3.60 water molecules and forms 3.02 hydrogen bonds with these water molecules. In bulk SPC/E water, each water molecule is coordinated with 4.40 water molecules and forms 3.60 hydrogen bonds with them. These data show that, although each water molecule in the channel is coordinated by less water molecules due to confinement, the hydrogen bonding network between water molecules is little weaken since each water molecule forms hydrogen bonds with a slightly higher fraction of its coordination water molecules than in the bulk. The water molecules inside the channel can form hydrogen bonds with a large fraction of their coordination water molecules by preferentially adopting configuration in which their dipoles (hence O-H bonds) are oriented parallel to the channel wall (see Fig. S5).

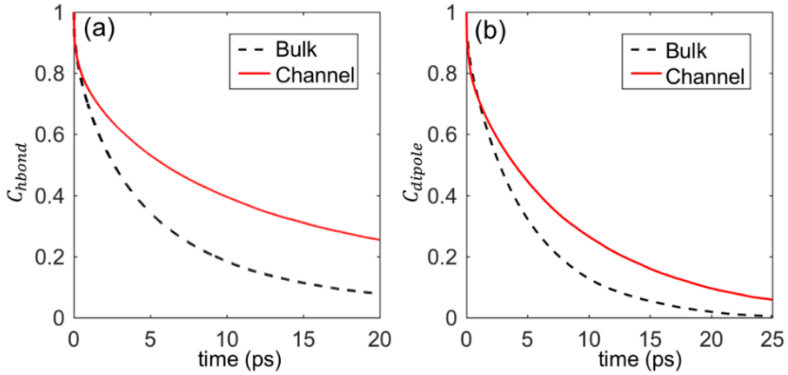

Figure 4. *Dynamics of quasi-2D water in 0.85nm-wide pristine graphene channels and bulk water.* (**a**) The intermittent hydrogen bond time autocorrelation function. (**b**) The water dipole moment autocorrelation function.

To further examine the dynamics of the hydrogen bonding between water molecules, we compute the intermittent hydrogen bond time autocorrelation function[40]

$$C_{hbond}(t) = \langle h(0)h(t)\rangle / \langle h(0)h(0)\rangle \quad (2)$$

where $h(t)$ is a binary function that equals to 1 if a pair of water molecules hydrogen bonded at time 0 is also hydrogen bonded at time *t*, and is 0 otherwise. Figure 4a shows that $C_{hbond}(t)$ decays much slower for the quasi-2D water confined in graphene channels than that for bulk water. This suggests that the hydrogen bonds between water molecules confined in the graphene channel break less easily than those in bulk, thus helping explain why the viscosity of the quasi-2D water is higher than that of the bulk water.

The slower rate for the hydrogen bonds in quasi-2D water to break compared with that in bulk water is closely related to the more sluggish rotation of water molecules in the channels. The breaking of hydrogen bonds often requires the rotation of water molecules. For water confined inside narrow channels, they are much less free to rotate than in bulk. As shown in Fig. 4b, the dipole moment correlation function decays much slower for water molecules confined in graphene channel than in bulk. Therefore, the sluggish rotation of water molecules helps explain the slower breakage of the hydrogen bonds in quasi-2D water and consequently the higher viscosity of such water.

C. Flow of Quasi-2D Water in graphene channels with surface hydroxyl groups

Prior works showed that, in graphene channels with width comparable to the water molecules' size, the functionalization groups on the graphene surface contribute greatly to the flow resistance through the channels.[19, 41] Below we investigate how these functionalization groups hinder the transport of quasi-2D water through graphene channels. Because the functionalization groups on graphene surfaces can either form mesoscale, oxygen rich domains[20] or distribute rather randomly, these situations are considered separately. We only consider hydroxyl groups, a common type of surface functionalization group. We first consider the flow near hydroxyl clusters, with a focus on how the flow field is perturbed by the hydroxyl cluster and the drag exerted to water by the cluster.

To understand how hydroxyl groups affect the transport of quasi-2D water through graphene channels, clusters containing 1, 3, 6, and 12 hydroxyl groups are anchored at the center of the lower wall of 0.85nm-wide graphene channels. In each cluster, the spacing between the

neighboring hydroxyl groups is ~0.24nm, which is close to that for GO sheets with uniformly distributed hydroxyl group at an O/C ratio of 0.5. The lateral dimension of the graphene walls is 12.18 and 12.12nm in the *x*- and *y*-directions, respectively. The MD box length is ~50 times of the radius of one hydroxyl group (0.23nm, see below). A constant acceleration of g_x=1×10^{-3} nm/ps^2 is applied on all water molecules in the channel to drive flow in the *x*-direction. Separate simulations confirmed that the flow response is in the linear regime with the acceleration used here.

We first examine the structure and flow of water near a single hydroxyl group. Figure 5a shows the water number density distribution in the *xy*-plane around the hydroxyl group. The hydroxyl group is hydrated by a ring of water molecules around it and water shows no clear structure at a radial distance larger than ~0.5nm. The lower water density in the ring center is due to the excluded volume by the hydroxyl group.[42] Figure 5b further shows the water number density distribution around the hydroxyl group in the radial (*r*-) and height (*z*-) directions (the carbon atom connected to this hydroxyl group is located at (*r*, *z*) = (0, 0)). The significant peak at (*r*, *z*) = (0.23nm, 0.32nm) indicates that the hydroxyl group is hydrated mostly by the water molecules in the same *z*-plane. Based on the lateral position of its nearest hydration peak, the effective radius of a single hydroxyl group can be taken as 0.23nm. The weak peak at (*r*, *z*) = (0.0nm, 0.52nm) indicates that some water molecules can also access the space above the hydroxyl group.

The hydroxyl group protruding into the channel hinders the water transport through the channel. For the flow around a single hydroxyl group considered here, Fig. 5c-d shows the water velocity in *x*-direction (u_x) along two strips passing through the hydroxyl group (cf. strips 1 and 2 in Fig.5a). The velocity of water is reduced notably below the upstream velocity at distances up to ~5nm from the hydroxyl group. Nevertheless, an approximately uniform velocity of $U_\infty = 19.8$m/s is reached at position ~6nm upstream of the hydroxyl group (see Fig. 5d). Using a radius of $R = 0.23$nm for the hydroxyl group and a kinematic viscosity of ν =1.09×10^{-6}m^2/s for the quasi-2D water, the Reynolds number for the flow around the hydroxyl group can be estimated as $Re = 2U_\infty R/\nu = 8.34 \times 10^{-3}$. Figure 5 c-d show that fluid flow is perturbed by a hydroxyl group at position tens of its radius. For larger hydroxyl clusters, flow is also retarded in a wide region around them (see Fig. 6b). For example, within the simulation box that spans ~12nm in both *x*- and *y*-directions, the velocity is distinctly non-uniform even at the furthest position from the cluster featuring 3 hydroxyl groups (see Fig. S6 in the Supplementary Material). The difficulty in reaching uniform fluid

velocity away from the hydroxyl cluster is consistent with the theories and simulations of low-Reynolds number flow in 2D space. For example, based on a recent study of such flows using Lattice Boltzmann simulations,[43] a uniform velocity at the far field can be rigorously achieved only when the MD box length reaches more than hundreds of nanometers. However, the finite box size has a weak effect on the drag computed for a single hydroxyl group based on the Reynolds number and box size used in this study according to the systematic study in Ref. 43.

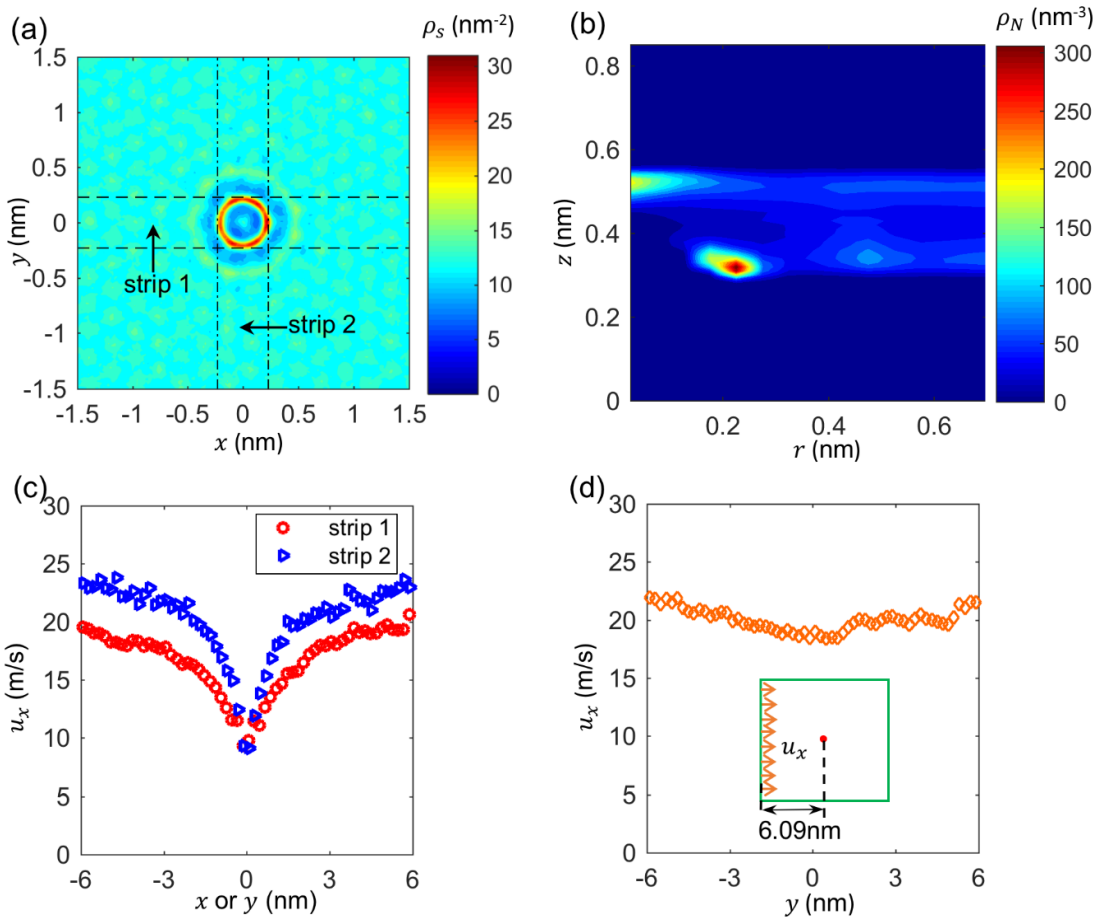

Figure 5. *Structure and flow of quasi-2D water near an isolated hydroxyl group on the lower wall of a pristine graphene channel*. (**a**) Water number density distribution around the hydroxyl group in the *xy*-plane. (**b**) The number density contour of water molecules around the hydroxyl group in the *rz*- plane. The carbon atom to which the hydroxyl group is anchored is located at (*x, y*) = (0nm, 0nm) and *r*- is the radial direction in the *xy*-plane emanating from this carbon atom and *z* is the distance from the lower graphene surface. (**c**) The *x*-direction velocity of water molecules along the two stripes labeled in panel **a**. (**d**) The *x*-direction velocity of water molecules from 6.09nm upstream of the hydroxyl group. In the inset, the green box denotes the simulation box measuring 12.18×12.12nm^2 in the *xy*-plane and the red dot denotes the hydroxyl group on the lower graphene wall.

An interesting observation of Fig. 5c-d is that, at the interface between the hydroxyl group and its hydration water, the water velocity drops to ~50% of the upstream velocity but never reaches zero. The latter indicates that both the water molecules sandwiched between the hydroxyl group and the upper graphene wall and the water molecules at the lateral side of the hydroxyl group maintain considerable velocity. Therefore, the no-slip boundary condition is not applicable to the flow around a single hydroxyl group anchored on the wall of the graphene channel considered here. For the larger hydroxyl clusters considered here, the spacing between neighboring hydroxyl groups is large enough that water molecules can penetrate into the interstitial space between the hydroxyl groups (see Fig. 6a). Figure 6b shows that water molecules can slip along the molecular surface of individual hydroxyl groups and flow through the space between the hydroxyl groups on the bottom graphene wall and the upper graphene wall. This result suggests that small patches of hydroxyl groups on graphene walls, while slowing down the water transport in the channel, does not eliminate the flow even when the spacing between neighboring hydroxyl groups (~0.24nm in the present study) is close to the size of a water molecule.

It is desirable to compare the MD velocity field with the prediction by the 2D hydrodynamics. However, this comparison is difficult for two reasons. First, although the flow away from the cluster is essentially 2D, the flow near the cluster does have 3D features. For example, there are water molecules between the hydroxyl group and the upper channel wall (see Fig. 5b) and thus the hydroxyl group cannot be taken as an infinite cylinder as in 2D hydrodynamics. Second, the water molecules in contact with the hydroxyl group have finite velocity (see Fig. 5c), and thus what boundary condition to apply on the hydroxyl group's surface in continuum calculation is not clear.

The hydroxyl cluster retards the flow by exerting a drag force ($F_{d,hdrx}$) to the water. Following the practice in continuum hydrodynamics, we characterize this drag by dividing it by the free stream velocity U_∞ (i.e., the average fluid velocity at position 6nm far away from the cluster, where the flow is little disturbed). $F_{d,hdrx}$ is computed using $F_{d,hdrx} = F_{d,tot} - F_{d,gn}$, where $F_{d,tot}$ is the total drag force experienced by water (which is equal to the external force applied to the water) and $F_{d,gn}$ is the drag rendered by the pristine portion of the channel walls. Although our simulation box is quite large in the horizontal plane (12.18×12.12nm^2), a somewhat uniform velocity at position away from the cluster is approximately reached only when the cluster contains one hydroxyl group. Since the area occupied by a single hydroxyl group is negligible compared to

the total area of the graphene walls, $F_{d,gn}$ is computed using $F_{d,gn} = A\overline{U}f_{w,pris}$, where A is the projection area of the graphene wall, $f_{w,pris}$ is the friction factor computed earlier for pristine graphene walls (1.23×10^4 Pa·s/m), and $\overline{U}$ is the average velocity of the water molecules in the slit channel. Using the above method, $F_{d,hdrx}/U_\infty$, is determined as 1.06×10^{-12} N·s/m for a single, isolated hydroxyl group, i.e., the drag rendered by an isolated hydroxyl group is equivalent to that by pristine graphene walls with a projection area of $F_{d,hdrx}/(U_\infty f_{w,pris}) = 86.2\,\text{nm}^2$. Clearly, surface functionalization groups, even though they may occupy little area on the graphene walls, can render significant drag to the quasi-2D water. As shown below, $F_{d,hdrx}/U_\infty$ is useful for determining how the flow in graphene channels is hindered by randomly distributed hydroxyl groups on the graphene walls.

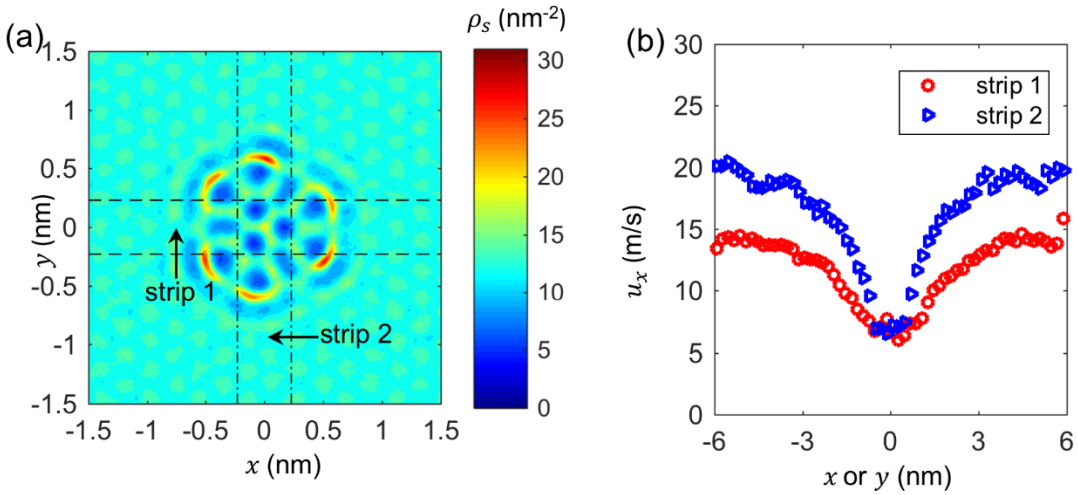

Figure 6. *Structure and flow of quasi-2D water near a cluster of 12 hydroxyl groups anchored on the lower wall of a pristine graphene channel*. (**a**) Water number density distribution around the hydroxyl group in the *xy*-plane. (**b**) The *x*-direction velocity of water molecules along the two stripes labeled in panel **a**.

For practical applications such as desalination, it is useful to know how flow through graphene channels is hindered by graphene wall and the functionalization groups on them in addition to the detailed flow characteristics described above. For a given channel width, such hindrance depends on the type, density, and distribution of the functionalization groups on the graphene walls. Below we study such hindrance by computing the drag rendered by the graphene walls and their functionalization groups to quasi-2D water when graphene walls are functionalized with randomly distributed hydroxyl groups. The channel width is the same as above (0.85nm) and the area density of the hydroxyl groups, c_s, is kept below 2nm^{-2}. Note that c_s is measured as the number of

hydroxyl groups in contact with water per unit projection area of the graphene walls. The hydroxyl groups are functionalized on both sides of each graphene walls as shown in Fig. 1b and a c_s less than 2nm^{-2} corresponds to an O/C ratio of less than 0.05 for the graphene walls.

To generate a flow through the channel, we apply an acceleration to all water molecules in the x-direction and measure the average velocity of the resulting flow, U_x. Because water is a quasi-2D fluid sandwiched by channel walls with surface functionalization groups, it is convenient to lump the channel walls and their functionalization groups together and characterize their hindrance to the flow using a friction factor f

$$f = F_d/AU_x \qquad (3)$$

where F_d is the total external force applied to the water molecules, which is equal to the drag force experienced by them. A is the projection area of the graphene walls in the horizontal plane.

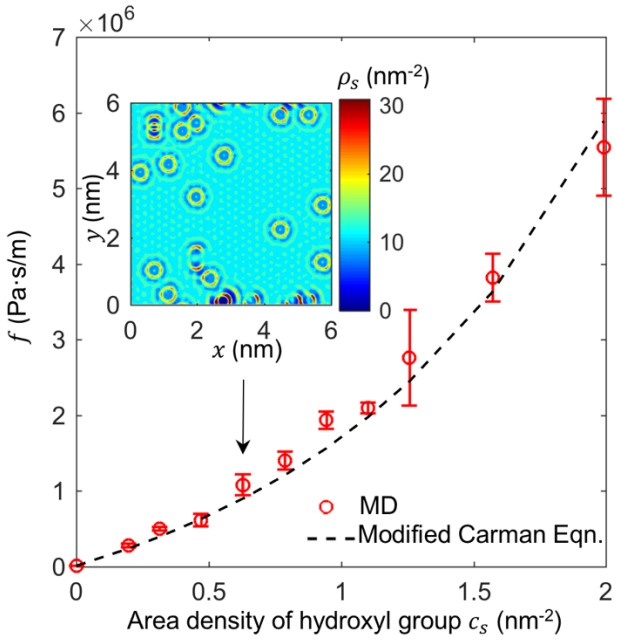

Figure 7. *The friction factor of graphene channel whose walls feature randomly distributed hydroxyl groups*. The channel width is 0.85nm. The inset is the water number density distribution in the *xy*-plane at a hydroxyl area density of 0.63nm^{-2}.

At hydroxyl area density $c_s = 0$ (i.e., pristine graphene walls), the friction factor f reduces to the friction factor of the pristine graphene channel: $f = f_{w,pris} = 1.23\times 10^4$ Pa·s/m. Figure 7 shows that the friction factor at different hydroxyl densities. For each density c_s, the friction factor and its error bar are obtained from four sets of simulations with independent initial configurations

of water molecules and randomly distributed hydroxyl groups on the graphene walls. Figure 7 shows that f increases rather linearly with c_s for $c_s \lesssim 0.5\text{nm}^{-2}$, largely because the flow near individual hydroxyl groups interacts weakly with each other. At $c_s > 0.5\text{nm}^{-2}$, hydroxyl groups approach each other rather closely and the regions in which water structure is altered by them start to overlap (see Fig. 7's inset). Hence, the flow near different hydroxyl groups affects each other markedly and the friction factor increases nonlinearly. Physically, as c_s increases, water molecules in the channel travel increasingly more tortuous pathways and interact with increasingly more hydroxyl groups as they move along the channel. Consequently, the friction factor increases sharply.

The friction factor shown in Fig. 7 allows one to calculate the flux of quasi-2D water through graphene channels without resolving the flow fields in the channel. This is similar to the calculation of fluid flux through porous media in continuum theories. Specifically, modeling of the flow in porous media often relies on homogenized models in which the flow field at the pore scale is not resolved explicitly but the drag force rendered by the solid matrix to the flow is described using empirical laws. For example, the drag by a porous solid matrix to the fluids in it is often described using the Carman equation $\mathfrak{D} = a\phi(1-\phi)^{-3}u$, where $\mathfrak{D}$ is the volumetric drag, ϕ is the solid volume fraction, u is the local fluid velocity, and a is a constant.[44] Since the flow through graphene channels in which surface hydroxyl groups protrude into the channel interior is similar to the flow through a packed bed of solid particles, in spirit of the classical Carman equation, we fit the data in Fig. 7 to a modified Carman equation

$$f(\theta) = f_{w,pris}(1-\theta) + k\theta(1-\theta)^{-3} \qquad (4)$$

where $\theta = c_s\pi r_h^2$ is the surface fraction of the hydroxyl groups, r_h is the hydrodynamic radius of individual hydroxyl groups, and k is a constant. The first and second terms account for the drag rendered by the pristine portion of graphene wall and the hydroxyl groups, respectively. With the drag rendered by pristine graphene and an isolated hydroxyl group obtained above ($f_{w,pris} = 1.23 \times 10^4$ Pa·s/m and $F_{d,hdrx}/U_\infty = 1.06 \times 10^{-12}$ N·s/m), the key fitting parameter is the hydrodynamic radius r_h of individual hydroxyl groups. Figure 7 shows that the computed friction factor can be fitted quite well to Eqn. 4 if r_h is taken as 0.22nm. This fitted r_h is reasonable since it is close to the distance between a hydroxyl group anchored on a graphene wall and the first ring of water molecules around it (see Fig. 5b). Thus, the friction factor and its scaling with the

functionalization groups' density for the flow of quasi-2D water through graphene channels can also be captured using the same form of empirical correlations used in continuum hydrodynamics.

IV. Conclusions

In summary, we study the structure, dynamics, and flow of water in graphene channels slightly wider than the diameter of a single water molecule. In such narrow channels, water molecules are coordinated primarily by neighboring water molecules within the same horizontal plane, and water essentially becomes quasi-2D liquids. The flow of such quasi-2D liquids is dominated by in-plane shearing and the hindrance by surface functionalization groups protruding into the channel. We show that the flow of such quasi-2D liquids can be modeled using classical hydrodynamic models. The effective kinematic viscosity of the water confined in 0.85nm-wide channels with pristine graphene walls is ~50% higher than the bulk water, largely because of the slowed rotation of water molecules in the channel. The flow of such quasi-2D water around single and clusters of hydroxyl groups functionalized on the graphene walls exhibit features similar to continuum-scale low Re-number flows near immersed objects, e.g., the disturbance of flow by a cluster extends tens of cluster radius from the cluster center. When water molecules penetrate into the interstitial space between the hydroxyl groups, the no-slip boundary condition is not satisfied at the hydroxyl-water interface. Nevertheless, these groups render significant drag to the flow, e.g., an isolated hydroxyl group produces drag equivalent to ~90nm^2 of pristine graphene walls. Similar to the flow in porous media, the drag rendered by a graphene channel with randomly distributed surface hydroxyl groups can be characterized using an effective friction factor. For slit graphene channels with a width of 0.85nm, the friction factor increases linearly up to a hydroxyl surface density of ~0.5nm^{-2} (or equivalently an O/C ratio of 0.013). At higher surface densities, drag increases sharply and can be captured using a modified Carman equation at least up to a surface density of ~2nm^{-2} (O/C ratio of ~0.05).

Molecularly wide nanochannels formed by graphene sheets have many potential applications. Understanding the dynamic properties of fluids confined in such channels and how flow through these channels is affected by the properties of the graphene sheets is essential for applications such as water desalination and gas separation. Our study highlights that surface functionalization groups on the graphene walls dominate the drag on the water moving through these channels even at low functionalization densities. The quantitative insight on how hydroxyl groups screen flow helps

understand the water permeation through graphene membranes and guide their design for desalination. For example, because a single hydroxyl group renders drag equivalent to ~90nm^2 of pristine graphene to quasi-2D water confined in graphene channels and the carbon atom density of a single-layer graphene is ~39nm^{-2}, the O/C ratio of graphene walls with uniformly distributed hydroxyl groups should be less than $\sim 3 \times 10^{-4}$ for the channel to exhibit water transport comparable to pristine graphene channel. If hydroxyl groups are randomly distributed on graphene, their area density should ideally be controlled to <0.5nm^{-2} (or equivalently, an O/C ratio of less than ~0.013) since the drag rendered by them increases sharply at higher area densities.

SUPPLEMENTARY MATERIAL

See supplementary material for 3D views of the simulation system, method for determining the number of water molecules inside the channels, considerations of graphene flexibility and thermostatting in flow simulations, calculation of friction coefficient of pristine graphene wall, force field parameters, the orientation of water molecules inside pristine graphene channels, and the structure and flow of quasi-2D water near a cluster of three hydroxyl groups anchored on the lower wall of a graphene channel.

ACKNOWLEDGEMENT

We thank the ARC at Virginia Tech for generous allocations of computer time.

References

1. Sparreboom, W. v.; Van Den Berg, A.; Eijkel, J. Principles and applications of nanofluidic transport. *Nat. Nanotechnol.* **2009,** *4* (11), 713-720.
2. Bocquet, L.; Charlaix, E. Nanofluidics, from bulk to interfaces. *Chem. Soc. Rev.* **2010,** *39* (3), 1073-1095.
3. Eijkel, J. C.; Van Den Berg, A. Nanofluidics: what is it and what can we expect from it? *Microfluidics and Nanofluidics* **2005,** *1* (3), 249-267.
4. Karnik, R.; Duan, C.; Castelino, K.; Daiguji, H.; Majumdar, A. Rectification of ionic current in a nanofluidic diode. *Nano Lett.* **2007,** *7* (3), 547-551.
5. Li, L.; Mo, J.; Li, Z. Nanofluidic diode for simple fluids without moving parts. *Phys. Rev. Lett.* **2015,** *115* (13), 134503.
6. Kleinstreuer, C. *Microfluidics and nanofluidics: theory and selected applications*; John Wiley & Sons, 2013.
7. Qiao, R.; Aluru, N. Atypical dependence of electroosmotic transport on surface charge in a single-wall carbon nanotube. *Nano Lett.* **2003,** *3* (8), 1013-1017.

8. Chen, Y.; Ni, Z.; Wang, G.; Xu, D.; Li, D. Electroosmotic flow in nanotubes with high surface charge densities. *Nano Lett.* **2007,** *8* (1), 42-48.
9. Barisik, M.; Beskok, A. Molecular dynamics simulations of shear-driven gas flows in nano-channels. *Microfluidics and nanofluidics* **2011,** *11* (5), 611-622.
10. Karniadakis, G.; Beskok, A.; Aluru, N. Water in Nanochannels. *Microflows and Nanoflows: Fundamentals and Simulation* **2005**, 407-445.
11. Zhu, Y.; Granick, S. Viscosity of interfacial water. *Phys. Rev. Lett.* **2001,** *87* (9), 096104.
12. Babu, J. S.; Sathian, S. P. The role of activation energy and reduced viscosity on the enhancement of water flow through carbon nanotubes. *J. Chem. Phys.* **2011,** *134* (19), 194509.
13. Travis, K. P.; Todd, B.; Evans, D. J. Departure from Navier-Stokes hydrodynamics in confined liquids. *Phys. Rev. E* **1997,** *55* (4), 4288.
14. Todd, B.; Hansen, J.; Daivis, P. J. Nonlocal shear stress for homogeneous fluids. *Phys. Rev. Lett.* **2008,** *100* (19), 195901.
15. Jiang, X.; Qiao, R. Electrokinetic transport in room-temperature ionic liquids: Amplification by short-wavelength hydrodynamics. *J. Phys. Chem. C* **2011,** *116* (1), 1133-1138.
16. Holt, J. K.; Park, H. G.; Wang, Y.; Stadermann, M.; Artyukhin, A. B.; Grigoropoulos, C. P.; Noy, A.; Bakajin, O. Fast mass transport through sub-2-nanometer carbon nanotubes. *Science* **2006,** *312* (5776), 1034-1037.
17. Nair, R.; Wu, H.; Jayaram, P.; Grigorieva, I.; Geim, A. Unimpeded permeation of water through helium-leak–tight graphene-based membranes. *Science* **2012,** *335* (6067), 442-444.
18. Yoshida, H.; Bocquet, L. Labyrinthine water flow across multilayer graphene-based membranes: Molecular dynamics versus continuum predictions. *J. Chem. Phys.* **2016,** *144* (23), 234701.
19. Wei, N.; Peng, X.; Xu, Z. Breakdown of fast water transport in graphene oxides. *Phys. Rev. E* **2014,** *89* (1), 012113.
20. Wei, N.; Peng, X.; Xu, Z. Understanding water permeation in graphene oxide membranes. *ACS Appl. Mater. Interfaces* **2014,** *6* (8), 5877-5883.
21. Chen, B.; Jiang, H.; Liu, X.; Hu, X. Observation and Analysis of Water Transport through Graphene Oxide Interlamination. *J. Phys. Chem. C* **2017,** *121* (2), 1321-1328.
22. Neek-Amal, M.; Peeters, F. M.; Grigorieva, I. V.; Geim, A. K. Commensurability Effects in Viscosity of Nanoconfined Water. *ACS Nano* **2016,** *10* (3), 3685-3692.
23. Algara-Siller, G.; Lehtinen, O.; Wang, F.; Nair, R.; Kaiser, U.; Wu, H.; Geim, A.; Grigorieva, I. Square ice in graphene nanocapillaries. *Nature* **2015,** *519* (7544), 443-445.
24. Skowron, S. T.; Lebedeva, I. V.; Popov, A. M.; Bichoutskaia, E. Energetics of atomic scale structure changes in graphene. *Chem. Soc. Rev.* **2015,** *44* (10), 3143-3176.
25. Joly, L.; Tocci, G.; Merabia, S.; Michaelides, A. Strong Coupling between Nanofluidic Transport and Interfacial Chemistry: How Defect Reactivity Controls Liquid–Solid Friction through Hydrogen Bonding. *J. Phys. Chem. Lett.* **2016,** *7* (7), 1381-1386.
26. Zhu, Y.; Wang, F.; Bai, J.; Zeng, X. C.; Wu, H. Compression limit of two-dimensional water constrained in graphene nanocapillaries. *ACS Nano* **2015,** *9* (12), 12197-12204.

27. Raghav, N.; Chakraborty, S.; Maiti, P. K. Molecular mechanism of water permeation in a helium impermeable graphene and graphene oxide membrane. *Phys. Chem. Chem. Phys.* **2015,** *17* (32), 20557-20562.
28. Jorgensen, W. L.; Maxwell, D. S.; Tirado-Rives, J. Development and Testing of the OPLS All-Atom Force Field on Conformational Energetics and Properties of Organic Liquids. *J. Am. Chem. Soc.* **1996,** *118* (45), 11225-11236.
29. Falk, K.; Sedlmeier, F.; Joly, L.; Netz, R. R.; Bocquet, L. Molecular origin of fast water transport in carbon nanotube membranes: superlubricity versus curvature dependent friction. *Nano Lett.* **2010,** *10* (10), 4067-4073.
30. Kannam, S. K.; Todd, B.; Hansen, J. S.; Daivis, P. J. How fast does water flow in carbon nanotubes? *J. Chem. Phys.* **2013,** *138* (9), 094701.
31. Celebi, A. T.; Barisik, M.; Beskok, A. Electric field controlled transport of water in graphene nano-channels. *J. Chem. Phys.* **2017,** *147* (16), 164311.
32. Hess, B.; Kutzner, C.; van der Spoel, D.; Lindahl, E. GROMACS 4: Algorithms for Highly Efficient, Load-Balanced, and Scalable Molecular Simulation. *J. Chem. Theory Comput.* **2008,** *4* (3), 435-447.
33. Bussi, G.; Donadio, D.; Parrinello, M. Canonical sampling through velocity rescaling. *J. Chem. Phys.* **2007,** *126* (1), 014101.
34. Darden, T.; York, D.; Pedersen, L. Particle mesh Ewald: An N·log(N) method for Ewald sums in large systems. *J. Chem. Phys.* **1993,** *98* (12), 10089-10092.
35. Yeh, I.-C.; Berkowitz, M. L. Ewald summation for systems with slab geometry. *J. Chem. Phys.* **1999,** *111* (7), 3155-3162.
36. Kumar Kannam, S.; Todd, B.; Hansen, J. S.; Daivis, P. J. Slip length of water on graphene: Limitations of non-equilibrium molecular dynamics simulations. *J. Chem. Phys.* **2012,** *136* (2), 024705.
37. Kumar, P. V.; Bardhan, N. M.; Tongay, S.; Wu, J.; Belcher, A. M.; Grossman, J. C. Scalable enhancement of graphene oxide properties by thermally driven phase transformation. *Nat. Chem.* **2014,** *6* (2), 151-158.
38. Erickson, K.; Erni, R.; Lee, Z.; Alem, N.; Gannett, W.; Zettl, A. Determination of the local chemical structure of graphene oxide and reduced graphene oxide. *Adv. Mater. Weinheim.* **2010,** *22* (40), 4467-4472.
39. Wu, Y.; Tepper, H. L.; Voth, G. A. Flexible simple point-charge water model with improved liquid-state properties. *J. Chem. Phys.* **2006,** *124* (2), 024503.
40. Luzar, A.; Chandler, D. Hydrogen-bond kinetics in liquid water. *Nature* **1996,** *379* (6560), 55.
41. Xu, W. L.; Fang, C.; Zhou, F.; Song, Z.; Liu, Q.; Qiao, R.; Yu, M. Self-Assembly: A Facile Way of Forming Ultrathin, High-Performance Graphene Oxide Membranes for Water Purification. *Nano Lett.* **2017,** *17* (5), 2928-2933.
42. Giovambattista, N.; Debenedetti, P. G.; Rossky, P. J. Hydration behavior under confinement by nanoscale surfaces with patterned hydrophobicity and hydrophilicity. *J. Phys. Chem. C* **2007,** *111* (3), 1323-1332.

43. Khalili, A.; Liu, B. Stokes' paradox: creeping flow past a two-dimensional cylinder in an infinite domain. *J. Fluid Mech.* **2017,** *817*, 374-387.
44. Hill, R. J.; Saville, D.; Russel, W. Electrophoresis of spherical polymer-coated colloidal particles. *J. Colloid Interface Sci.* **2003,** *258* (1), 56-74.